Journal of
Materials Chemistry A

Accepted Manuscript

This article can be cited before page numbers have been issued, to do this please use: D. Yang, Y. Jiao, L. Yang, Y. Chen, S. Mizoi, Y. Huang, X. Pu, Z. Lu, H. Sasabe and J. Kido, *J. Mater. Chem. A*, 2015, DOI: 10.1039/C5TA03971A.

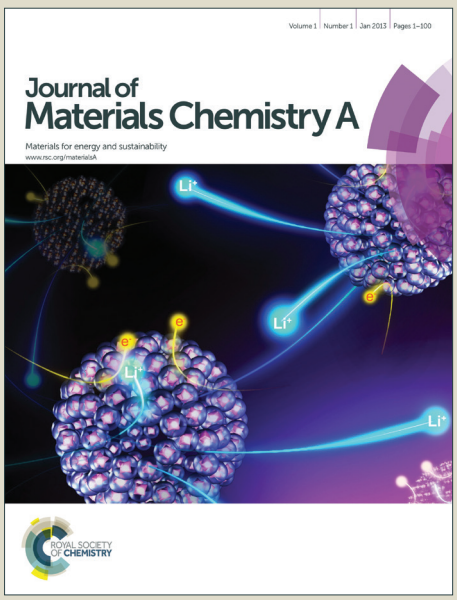

This is an *Accepted Manuscript*, which has been through the Royal Society of Chemistry peer review process and has been accepted for publication.

Accepted Manuscripts are published online shortly after acceptance, before technical editing, formatting and proof reading. Using this free service, authors can make their results available to the community, in citable form, before we publish the edited article. We will replace this *Accepted Manuscript* with the edited and formatted *Advance Article* as soon as it is available.

You can find more information about *Accepted Manuscripts* in the Information for Authors.

Please note that technical editing may introduce minor changes to the text and/or graphics, which may alter content. The journal's standard Terms & Conditions and the Ethical guidelines still apply. In no event shall the Royal Society of Chemistry be held responsible for any errors or omissions in this *Accepted Manuscript* or any consequences arising from the use of any information it contains.

ROYAL SOCIETY OF CHEMISTRY

www.rsc.org/materialsA

View Article Online
DOI: 10.1039/C5TA03971A

Cyano-Substitution on the End-Capping Group: A Facile Access toward Asymmetrical Squaraine Showing Strong Dipole-Dipole Interactions as High Performance Small Molecular Organic Solar Cells Material †

Daobin Yang,[a,b] Yan Jiao,[a] Lin Yang,[a] Yao Chen,[a] Satoshi Mizoi,[b] Yan Huang,*[a] Xuemei Pu,[a] Zhiyun Lu,[a] Hisahiro Sasabe*[b] and Junji Kido*[b]

[a] *Key Laboratory of Green Chemistry and Technology (Ministry of Education), College of Chemistry, Sichuan University, Chengdu 610064, People's Republic of China. E-mail: huangyan@scu.edu.cn*

[b] *Department of Organic Device Engineering, Research Center for Organic Electronics, Yamagata University, Yonezawa 992-8510, Japan. E-mail: h-sasabe@yz.yamagata-u.ac.jp; kid@yz.yamagata-u.ac.jp*

† Electronic supplementary information (ESI) available: electron density distribution and absorption spectra of the active layers.

Abstract: A novel asymmetrical squaraine derivative bearing cyano-substituted indoline end-capping group, namely ASQ-5-CN, was designed and synthesized. In comparison with the noncyano-substituted ASQ-5, ASQ-5-CN shown an analogous absorption band-gap in thin solid film state, but a 0.11 eV lowered HOMO energy level, which led to a higher V_{oc}. Density functional theory calculation results revealed that the dipole moment of ASQ-5-CN was 2 times larger than that of ASQ-5. Hence the stronger dipole-dipole interactions of ASQ-5-CN might trigger more intense intermolecular packing in ASQ-5-CN, which should account for the higher hole-mobility of ASQ-5-CN than that of ASQ-5 (4.00×10^{-5} *vs.* 1.67×10^{-5} cm^2 V^{-1} s^{-1}). Accordingly, solution-processed bulk-heterojunction small molecular organic solar cell using ASQ-5-CN as electron donor exhibited much higher PCE (5.24%) than that of the reference compound ASQ-5-based device (4.22%) due to its simultaneously enhanced V_{oc} (0.92 *vs.* 0.82 V), J_{sc} (11.38 *vs.* 10.94 mA cm^{-2}) and FF (0.50 *vs.* 0.47).

Additionally, the PCE of the ASQ-5-CN-based device could be improved to be as high as 6.11% when measured at 80 °C, which is the record PCE among the hitherto reported squaraine-based solution-processed bulk-heterojunction organic solar cells.

1. Introduction

Owing to the well-defined molecular structure and molecular weight, high purity and good batch to batch reproducibility of small molecular compounds, solution-processed bulk-heterojunction small molecular organic solar cells (BHJ-SMOSC) have been demonstrated to be a competitive alternative to their polymeric counterparts recently.[1-7] Among the numerous kinds of small molecular OSC materials, squaraines dyes have drawn much attention because they not only possess high molar extinction coefficients, but also show intense and broad absorption in Vis-NIR spectral regions.[8-20] Nevertheless, although many efforts have been devoted to the exploitation of novel squaraines for OSC applications, the performance of photovoltaic squaraines is still unsatisfactory. For example, the record power conversion efficiency (PCE) of solution-processed squaraine-based BHJ-OSC is only 5.50%, note that the squaraine compound used just possesses a symmetrical molecular structure with a D-A-D skeleton.[21]

In comparison with symmetrical squaraines (SSQ), asymmetrical ones (ASQ) bearing a D-A-D′ rather than D-A-D molecular skeleton should be more promising due to their better structural tunability.[22,23] Consequently, recently, we have devoted to the development of novel ASQ materials for BHJ-OSC applications, in which 1,1,2-trimethyl-1*H*-benzo[*e*] indole acts as the D subunit, squaric acid core acts as the A subunit, and 2,6-dihydroxyphenyl group acts as the D′ subunit.[24-27] Through delicate modulation on the end-capping group of the D′ segment, such as diisobutylamino, 9-carbazyl, diarylamino, tetrahydroquinoline and indoline, a series of ASQ materials were achieved, and one of them bearing an indoline end-capping subunit (named ASQ-5, molecular structure shown in Fig.1) displayed the highest photovoltaic performance (PCE=4.29%). These encouraging results indicate that ASQ derivatives could act as perspective OSC materials, and indoline unit could serve as quite promising end-capping unit to construct high performance photovoltaic

ASQ materials. However, the performance of ASQ-5-based BHJ-SMOSC was still inferior to that of the device using a SSQ compound as photovoltaic material,[21] which should be ascribed to its relatively low open-circuit voltage (V_{oc}, 0.81 V) stemming from the relatively high HOMO energy level of ASQ-5 (-5.09 eV).[25] Therefore, we aimed at the exploitation of ASQ-5 derivatives with lower HOMO energy level, so that enhanced V_{oc} could be expected.

Owing to the strong electron-withdrawing nature and linear geometry of cyano groups, cyano-substitution was a well-adopted strategy with regard to the lowering of HOMO energy levels of OSC electron donor materials.[28,29] Moreover, according to Cha's report, the cyano-modified conjugated polymer shown higher crystallinity than its unmodified counterpart, resulting in OSC with higher fill factor (FF) and PCE.[30] However, most of the current studies have been focused on the cyano-substitution on the vinylic linkage of the molecular skeleton of photovoltaic materials and the dicyanovinyl-substituted compounds,[31-36] yet never concern has been paid on the effect of cyano-substitution on the end-capping groups in OSC. Consequently, a new asymmetrical squaraine (named ASQ-5-CN, molecular structure shown in Fig.1) bearing a cyano-substitution on the indoline end-capping unit of ASQ-5 was designed and synthesized, and the substitution effect of the cyano group on the end-capping segment of ASQ compounds has been investigated.

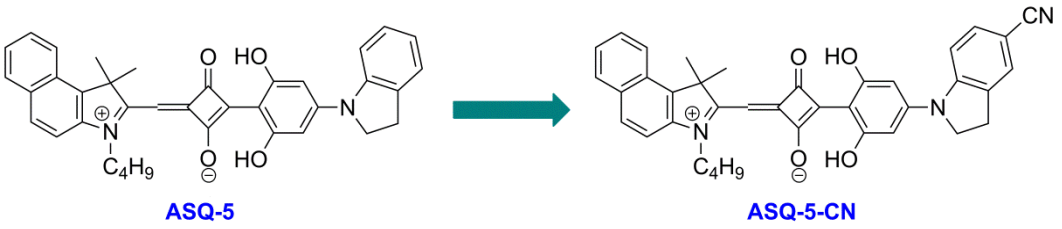

Fig. 1 Molecular structures of ASQ-5 and ASQ-5-CN.

2. Experimental section

2.1 Instruments and characterization

^{1}H NMR and ^{13}C NMR spectra were measured using a Bruker Avance AV II-400 MHz spectrometer, and the chemical shifts were recorded in units of ppm with TMS as the

internal standard. High resolution mass spectrum was obtained from a Shimadzu LCMS-IT-TOF. Thermogravimetry analysis (TGA) was performed on a Perkin-Elmer TGA Q500 instrument in an atmosphere of N_2 at a heating rate of 10 °C min^{-1}. The purity of ASQ-5-CN was measured by high performance liquid chromatography (EZChrom Elite, Hitachi, equipped with DAD and RI detectors). Electronic absorption spectra of both solution and thin-film samples of the two ASQs were recorded using a Perkin Elmer Lamdba 950 UV-Vis scanning spectrophotometer. The ground-state geometries and electronic structures of the two ASQs were calculated with Gaussian 09 software, using density functional theory (DFT) based on B3LYP/6-31G(d) and B3LYP/ 6-311G(d, p) levels. The solution samples were prepared in chloroform solution at a concentration of 3.0 $\times 10^{-6}$ mol L^{-1}, while the film samples were obtained by spin-coating from chloroform solution (4 mg mL^{-1}, 1500 rpm/ 45 s) on quartz substrates. Cyclic voltammetry (CV) measurement was carried out in 2.5×10^{-4} mol L^{-1} anhydrous dichloromethane (DCM) with tetrabutyl ammonium perchlorate (Bu_4NClO_4) under an argon atmosphere at a scan rate of 50 mV s^{-1} using a LK 2005A electrochemical workstation. The CV system was constructed using a Pt disk, a Pt wire, and a $Ag/AgNO_3$ (0.1 mol L^{-1} in acetonitrile) electrode as the working electrode, counter electrode and reference electrode, respectively, and the potential of the $Ag/AgNO_3$ reference electrode was internally calibrated with the ferrocene/ ferrocenium redox couple (Fc/Fc^+), which has a known reduction potential of -4.80 eV relative to vacuum level. The morphologies of the active layers were analyzed through atomic force microscopy (AFM) in tapping mode in air under room temperature using Bruker instrument, the active layers were fabricated on ITO/ MoO_3 (8 nm) substrates.

2.2 Device Preparation and characterization

Small molecular bulk-heterojunction organic solar cells were fabricated using indium-tin-oxide (ITO) coated glass as substrate. The sheet resistance of ITO is 15 Ω sq^{-1}. Patterned ITO-coated glass substrates were sequentially cleaned using detergent, deionized water, acetone, and isopropanol in an ultrasonic bath for 20 min each. The cleaned substrates were dried in an oven at 65 °C for 12 h before use. The substrates were treated by UV-ozone for 20 min, then immediately transferred into a high vacuum chamber for deposition of 8 nm

MoO_3 at a pressure of less than 1×10^{-4} Pa with a rate of 0.2 Å s^{-1}. Subsequently, photoactive layers (thickness: 60 nm, 3000 rpm/ 45s) were fabricated by spin-coating a blend of the asymmetrical squaraines and $PC_{71}BM$ in chloroform with total concentration of 18 mg mL^{-1} in a N_2-filling glovebox at 25 °C. Finally, the substrates were transferred back to the high-vacuum chamber, where BCP (6 nm) and Al (100 nm) were deposited as the top electrode at pressures of less than 8×10^{-5} Pa with a rate of 0.20 Å s^{-1} and 2×10^{-4} Pa with a rate of 1.5~4.0 Å s^{-1}, respectively, resulting in a final OSC with the structure of ITO/MoO_3(8 nm)/ASQ:$PC_{71}BM$/ BCP(6 nm)/Al(100 nm). The active area of OSC cell is 9 mm^2. Current density-voltage (*J-V*) and external quantum efficiency (EQE) characterizations of organic solar cells were performed on a CEP-2000 integrated system manufactured by Bunkoukeiki Co. The integration of EQE data over an AM 1.5G solar spectrum yielded calculated J_{sc} values with an experimental variation of less than 5% relative to the J_{sc} measured under 100 mW cm^{-2} simulated AM1.5G light illumination. Hole-only and electron-only devices were fabricated with structures of ITO/MoO_3(8 nm)/ASQ(40 nm) or ASQ: $PC_{71}BM$(60 nm)/MoO_3(8 nm)/Al(100 nm) and ITO/ZnO(20 nm)/ASQ: $PC_{71}BM$(60 nm)/BCP(6 nm)/Al(100 nm), respectively.

2.3 Synthesis

Intermediate 4 and reference compound ASQ-5 were prepared according to the procedures described in the literature.[25] *n*-Butanol and toluene were distilled from sodium freshly prior to use. All other chemicals were obtained from commercial sources and used as-received without further purification.

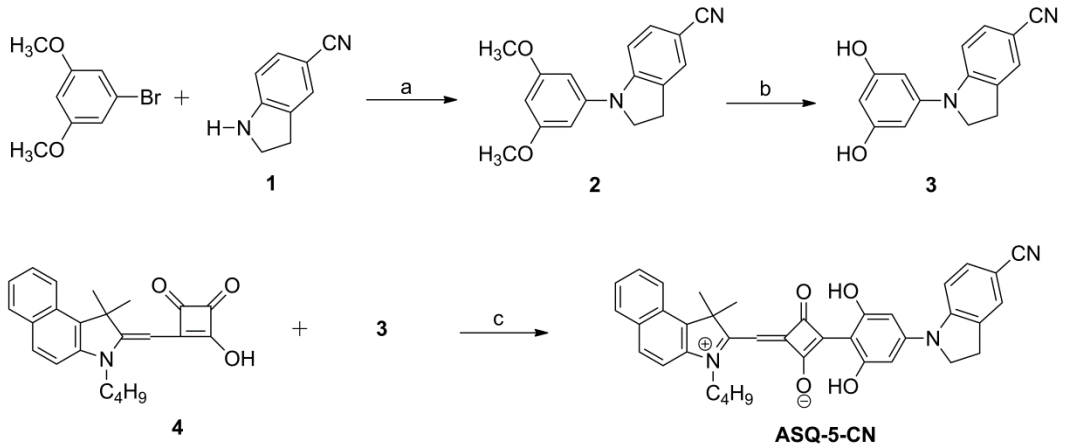

Scheme 1. Synthetic route to ASQ-5-CN. a) NaOBu-*t*, $Pd(OAc)_2$, $P(t\text{-}Bu)_3HBF_4$, toluene, reflux 12 h; b) BBr_3, DCM, r. t., 24 h; c) *n*-Butanol and toluene (1:1), 140 °C, 36 h.

5-Cyanoindoline (1).[37] To an acetic acid suspension (20 mL) of 5-cyanoindole (1.0 g, 6.94 mmol) was added $NaBH_3CN$ (2.62 g, 41.6 mmol) under 25 °C. The mixture was stirred at room temperature for one day. After the reaction was completed, the reaction mixture was poured into icy 4 M aqueous NaOH solution until a strongly basic pH was obtained. The crude product was extracted with dichloromethane, evaporated under vacuum, and purified by silica gel column chromatography (eluent: hexane/ ethyl acetate = 6:1) to afford compound 1 as a white solid (0.70 g, 69%). ^{1}H NMR (400 MHz, $CDCl_3$, ppm) δ: 7.31-7.29 (m, 2H, Ar H), 6.55 (d, 1H, *J*=8.0 Hz, Ar H), 3.69 (t, 2H, *J*=8.0 Hz, CH_2), 3.08 (t, 2H, *J*=8.0 Hz, CH_2).

1-(3,5-Dimethoxyphenyl)indoline-5-carbonitrile (2). A mixture of 1 (0.70 g, 4.79 mmol), 1-bromo-3,5-dimethoxybenzene (1.09 g, 5.03 mmol), NaOBu-*t* (sodium *tert*-butoxide) (0.69 g, 7.19 mmol), $Pd(OAc)_2$ (palladium (II) acetate) (22 mg, 1.5%), and $P(t\text{-}Bu)_3HBF_4$ (tri(*tert*-butyl)phosphine tetrafluoroborate) (56 mg, 4%) were dissolved in 50 mL of toluene and refluxed under Ar for 12 h. The reaction mixture was cooled down and filtered to remove insoluble material; then the solvents were removed under reduced pressure. The crude product was purified by silica gel column chromatography (eluent: hexane/ethyl acetate = 15:1) to afford compound 2 as a white solid (1.10 g, 89%). ^{1}H NMR (400 MHz, $CDCl_3$, ppm) δ: 7.36 (d, 2H, *J*=8.0 Hz, Ar H),7.07 (d, 1H, *J*=8.0 Hz, Ar H), 6.39 (d, 2H, *J*=2.0 Hz, Ar H), 6.22 (t, 1H, *J*=2.0 Hz, Ar H), 4.05 (t, 2H, *J*=8.4 Hz, NCH_2), 3.81 (s, 6H, OCH_3), 3.17 (t, 2H, *J*=8.4 Hz, CH_2); ^{13}C NMR (100 MHz, $CDCl_3$, ppm): δ: 161.6, 150.8, 144.1, 133.1, 132.0, 128.1, 120.4, 108.1, 100.5, 98.0, 95.0, 55.4, 52.6, 27.4; MS: *m/z* $[M+H]^+$ 281.2.

1-(3,5-Dihydroxyphenyl)indoline-5-carbonitrile (3). Compound 2 (1.0 g, 3.53 mmol) was added to 60 mL of anhydrous CH_2Cl_2, then boron tribromide (28 mL of 1 M solution in CH_2Cl_2, 28.2 mmol) was added dropwise slowly at ice bath. The solution was stirred under room temperature for 24 h, then was decanted to 100 mL of ice water to remove any excess BBr_3. The organic phase was separated, and the aqueous phase was extracted with CH_2Cl_2

(20 mL×3) for three times. The combined organic phases were washed with saturated aqueous $NaHCO_3$ solution and water in sequence, then dried over anhydrous Na_2SO_4. After removing solvent under vacuum, a yellow solid compound 3 (0.80 g, 89%) was obtained. Compound 3 was used to the next step reaction without further purification.

4-((3-Butyl-1,1-dimethyl-1H-benzo[*e*]indol-3-ium-2-yl)methylene)-2-(4-(5-cyanoindolin-1-yl)-2,6-dihydroxyphenyl)-3-oxocyclobut-1-enolate (**ASQ-5-CN**). A mixture of compound 4 (790 mg, 2.20 mmol) and 3 (700 mg, 3.75 mmol) in *n*-butanol (50 mL) and toluene (50 mL) were added into a round bottom flask. The mixture was refluxed with a Dean-Stark apparatus for 36 h. After the reactant was cooled down, the solvent was removed under reduced pressure. The resulting crude product was purified by silica gel column chromatography using dichloromethane/methanol (50:1, v/v) as the eluent to afford green solid. The solid was recrystallized from dichloromethane and methanol mixture (1:6, v/v) to afford green crystals of ASQ-5-CN (830 mg, 63%). M.p. 276-277 °C. ^{1}H NMR (400 MHz, $CDCl_3$, ppm) δ: 12.29 (s, 2H, OH), 8.24 (d, 1H, J=8.8 Hz, Ar H), 7.99 (d, 2H, J=8.8 Hz, Ar H), 7.69 (t, 1H, J=8.0 Hz, Ar H), 7.57 (t, 1H, J=7.6 Hz, Ar H), 7.45-7.35 (m, 4H, Ar H), 6.28 (d, 2H, J^3=3.2 Hz, Ar H), 6.09 (s, 1H, CH), 4.31 (t, 2H, J=7.2 Hz, NCH_2), 4.11 (t, 2H, J=8.4 Hz, NCH_2), 3.19 (t, 2H, J=8.4 Hz, CH_2), 2.05 (s, 6H, CH_3), 1.95-1.87 (m, 2H, CH_2), 1.57-1.48 (m, 2H, CH_2), 1.05 (t, 3H, J=7.2 Hz, CH_3); ^{13}C NMR (100 MHz, $CDCl_3$, ppm): δ: 184.0, 180.8, 177.1, 172.2, 168.1, 162.7, 162.2, 150.4, 148.5, 138.3, 136.8, 133.4, 132.9, 132.4, 130.6, 129.9, 128.3, 128.2, 128.1, 126.0, 122.8, 119.9, 111.6, 110.6, 105.1, 102.8, 97.6, 97.5, 88.7, 52.7, 52.2, 45.0, 30.0, 27.3, 26.2, 20.3, 13.8; purity: 100% (HPLC, eluent: THF/ CH_3OH=1:9); HR-MS (ESI): *m/z* $[M+H]^+$ calcd. for $C_{38}H_{34}N_3O_4$, 596.2549; found, 596.2548; Anal. calcd for $C_{38}H_{34}N_3O_4$: C 76.62, H 5.58, N 7.05; found, C 76.72, H 5.55, N 6.98.

3. Results and Discussion

3.1 Synthesis and characterization

The synthetic route to ASQ-5-CN was illustrated in Scheme 1. Intermediate 1-(3,5-dimethoxy-phenyl)indoline-5-carbonitrile (2) was prepared by Buchwald-Hartwig

reaction using 1-bromo-3,5-dimethoxybenzene and 5-cyanoindoline as reactants. Then the methoxy groups of compound 2 was deprotected in the presence of BBr_3 to afford intermediate 1-(3,5-dihydroxyphenyl)indoline-5-carbonitrile (3), which was further condensed with compound 4 to afford the objective compound ASQ-5-CN with a satisfactory yield of 63%. The solubility of ASQ-5-CN was found to be much inferior to that of the reference compound ASQ-5 in common organic solvents (*e.g.*, 6 *vs.* 40 mg mL^{-1} in chloroform), indicating that the cyano-substituted ASQ-5-CN possessed much stronger intermolecular interactions than ASQ-5. As shown in Fig. 2, ASQ-5-CN displayed a higher decomposition temperature (Table 1) than that of ASQ-5, indicative of the enhanced thermal stability of ASQ compounds upon cyano-modification.

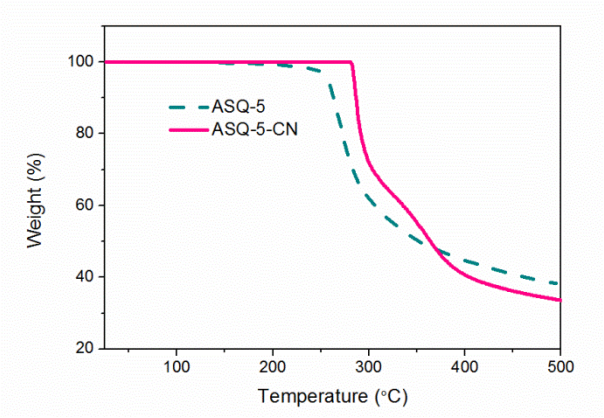

Fig. 2 TGA curves of the two compounds.

3.2 Optical properties

The UV-Vis absorption spectra of the two ASQ in dilute chloroform solution and thin film states were shown in Fig. 3, and data were summarized in Table 1. Similar to ASQ-5, the cyano-substituted compound ASQ-5-CN also shown intense absorption at 550~700 nm in dilute solution, with considerably high molar extinction coefficient of > 10^5 M^{-1} cm^{-1}. In dilute solution, the maximum absorption wavelength of ASQ-5-CN was blue-shifted for 14 nm than that of ASQ-5, which might arise from the lessened electron-donating capability of the end-capping group due to the presence of an electron-deficient cyano group in this compound. In comparison with their dilute solution samples, both ASQ-5-CN and ASQ-5 shown much bathochromic-shifted and broadened absorption spectra in thin solid film state,

but ASQ-5-CN shown a more bathochromic-shifted (55 *vs*. 41 nm) and broadened (full width at half maxima, FWHM: 3791 *vs.* 3336 cm^{-1}) absorption spectrum than that of ASQ-5, which should be propitious to the harvesting of solar irradiation.[10] In fact, although in solution state, the λ_{absmax} of ASQ-5-CN was 14 nm blue-shifted than that of ASQ-5 and the FWHM of the two compounds were identical (~ 900 cm^{-1}), the solid film samples of both ASQ-5-CN and ASQ-5 displayed an analogous absorption maximum of 718 nm. Consequently, there may be exist more intense intermolecular π-π stacking interactions in ASQ-5-CN than ASQ-5.[38] Determined from the onset position of the absorption spectra of the two ASQ in thin films, the optical band-gaps of ASQ-5-CN and ASQ-5 were both 1.43 eV.

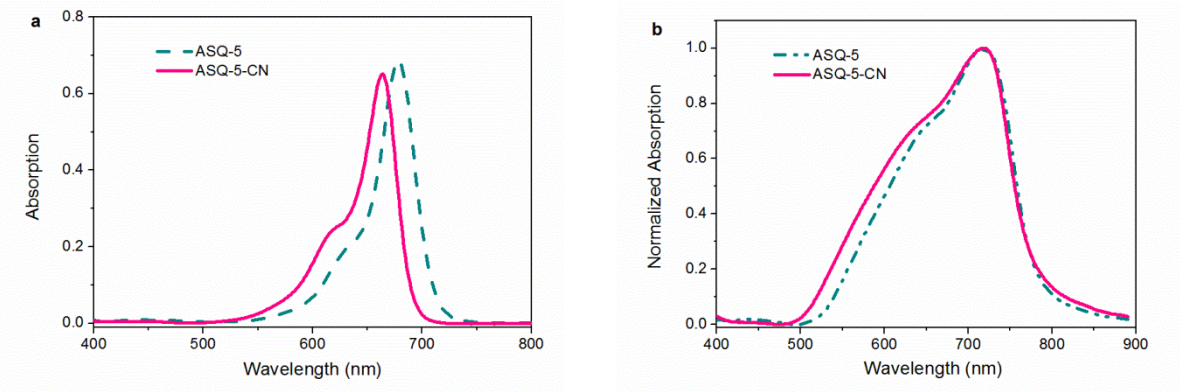

Fig. 3 Absorption spectra of the two compounds in a) dilute chloroform solution; and b) thin film states.

Table 1 Optical properties of the two compounds.

Compound	Absorption λ_{absmax} (nm)		FWHM (cm^{-1})		E_g^{opt}	T_d
	Solution ($\varepsilon \times 10^5$ M^{-1} cm^{-1})	Film	Solution	Film	(eV)	(°C)
ASQ-5	677 (2.29)	718, 656	876	3336	1.43	256
ASQ-5-CN	663 (2.18)	718, 646	922	3791	1.43	286

3.3 Electrochemistry properties

To estimate the energy level of ASQ-5-CN, its electrochemical property was investigated by cyclic voltammetry. As shown in Fig. 4 and Table 2, during anodic scan, a quasireversible oxidation process could be observed in ASQ-5-CN, and its E_{ox}^{onset} was determined to be 0.40

V relative to Fc/Fc^+. Hence, by comparison with the Fc/Fc^+ redox couple whose energy level is –4.80 eV in vacuum, the HOMO energy level of ASQ-5-CN was calculated to be –5.20 eV, which is 0.11 eV lower than that of ASQ-5 (–5.09 eV). Consequently, the introduction of a cyano substitution on the indoline end-capping segment could endow ASQ-5 derivatives with lower HOMO energy level, which could be beneficial to the enhancement of V_{oc} in their corresponding OSC device.[39] Moreover, deduced from the HOMO level and the corresponding optical band-gap, the LUMO energy level of ASQ-5-CN was calculated to be –3.77 eV, which was also 0.11 eV lower than that of ASQ-5, hence lower energy loss could be expected during the electron transfer processes from the ASQ donors to the $PC_{71}BM$ acceptor.[39]

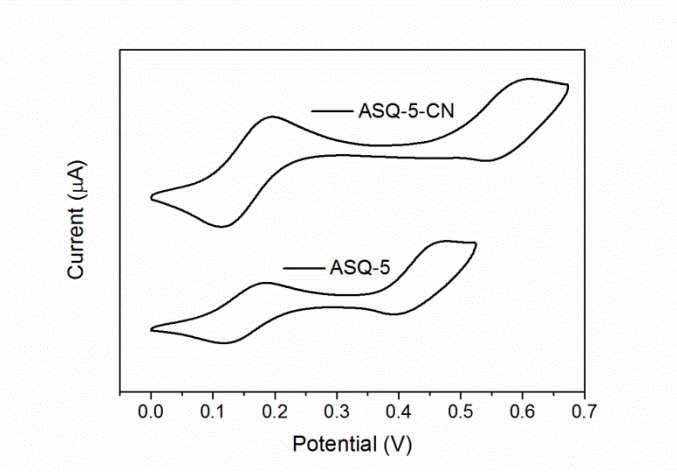

Fig. 4 Cyclic voltammogram of the two compounds.

Table 2 Cyclic voltammetry and DFT calculated data for the two compounds.

Compound	E_{ox}^{onest} (V)	HOMO [a] (eV)	LUMO [b] (eV)	HOMO [c] (eV)	LUMO [c] (eV)	μ_g [c] (D)
ASQ-5	0.29	–5.09	–3.66	–5.17	–2.94	3.73
ASQ-5-CN	0.40	–5.20	–3.77	–5.33	–3.06	11.26

[a] HOMO values derived from CV measurements; [b] LUMO = E_g^{opt} + HOMO; [c] data derived from DFT calculation.

3.4 DFT calculation

To gain further insights into the effects of cyano-substitution on the electronic properties of ASQ-5-CN, DFT calculations were performed on ASQ-5-CN and ASQ-5, and computational results were shown in Table 2, and the electron density distribution of the HOMO and LUMO of the two ASQ compounds were shown in Fig. S1 (ESI). According to the calculation results, the HOMO energy levels of ASQ-5 and ASQ-5-CN were –5.17 eV and –5.33 eV, respectively; while the LUMO energy levels of ASQ-5 and ASQ-5-CN were –2.94 eV and –3.06 eV, respectively. These data well reproduce their corresponding electrochemical characterization results, indicative of the reliability of the calculation results. More importantly, as shown in Fig. 5, both the two ASQ derivatives shown similar direction of dipole moment, however, ASQ-5-CN exhibited 2 times larger dipole moment than that of ASQ-5 (11.26 *vs.* 3.73 D), indicating that significantly stronger dipole-dipole interactions should exist in ASQ-5-CN, which may endow the compound with more enhanced higher hole mobility.[40-42] To the best of our knowledge, this is the first time to reveal that the cyano-substitution would result in increased dipole moment of the OSC materials. This finding should be great importance for the recognition of the role cyano-substitution might play in the rational molecular design of photovoltaic materials.

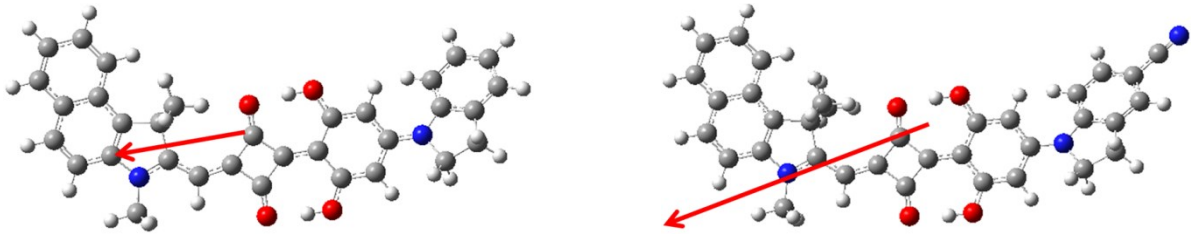

Fig. 5 The dipole moments of ASQ-5 (left) and ASQ-5-CN (right).

3.5 Hole and electron mobilities

The mobility of the two pristine ASQ as well as the ASQ/$PC_{71}BM$ (1:3, wt%) blend film samples were evaluated by the space charge limited current (SCLC) method,[43] and the results were shown in Table 3. The hole mobility of the neat ASQ-5-CN film was calculated to be 4.00 $\times 10^{-5}$ cm^2 V^{-1} s^{-1}, 2.4 times higher than that of ASQ-5 film (1.67 $\times 10^{-5}$ cm^2 V^{-1} s^{-1}). Besides, the hole (μ_h) and electron (μ_e) mobilities of ASQ-5-CN/$PC_{71}BM$ blend film were calculated to be 3.46 $\times 10^{-5}$ and 7.74 $\times 10^{-5}$ cm^2 V^{-1} s^{-1}, respectively, also higher than that of

ASQ-5/$PC_{71}BM$ blend films (1.30×10^{-5} and 4.56×10^{-5} cm^2 V^{-1} s^{-1}, respectively). Thus, ASQ-5-CN/$PC_{71}BM$ blend film (μ_e/μ_h=2.2) showed better balanced hole and electron mobilities than that of ASQ-5/$PC_{71}BM$ blend film (μ_e/μ_h=3.5). Upon thermal annealing at 80 °C for 10 min, all of the mobilities were slightly increased (*vide.* Table 3). In addition, when the carrier mobility measurement was tested at 80 °C, the hole and electron mobilities of the ASQ-5-CN/$PC_{71}BM$ blend film drastically increased to 11.0×10^{-5} and 13.5×10^{-5} cm^2 V^{-1} s^{-1}, respectively, and the μ_e/μ_h ratio decreased from 2.2 to 1.2, which is useful for enhanced J_{sc} and FF.[20] Both neat films and blend films, the ASQ-5-CN-based samples shown much higher hole mobility than that of the corresponding ASQ-5 samples. Additionally, AFM characterization revealed that the ASQ-5/$PC_{71}BM$ and ASQ-5-CN/ $PC_{71}BM$ blend films shown similar morphologies with quite smooth surfaces (Fig. 6), both of their RMS were slightly increased under thermal annealing. Therefore, the much increased hole mobility of ASQ-5-CN-based samples can most likely be ascribed to its significantly higher dipole moment.

Table 3 Mobilities data of the two compounds. (μ: $\times 10^{-5}$ cm^2 V^{-1} s^{-1})

	μ_h [a]	μ_h [b]	μ_h [c]	μ_h [d]	μ_e [b]	μ_e [c]	μ_e [d]
ASQ-5	1.67	1.30	1.89	--	4.56	6.44	--
ASQ-5-CN	4.00	3.46	4.84	11.0	7.74	10.6	13.5

[a] neat films; [b] pristine blend films; [c] thermal annealed blend films; [d] device tested at 80 °C.

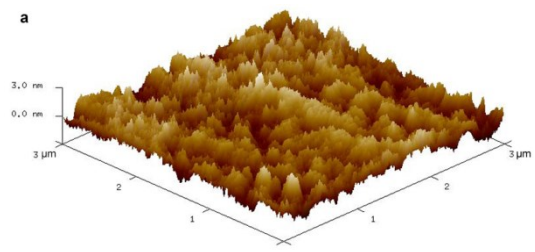

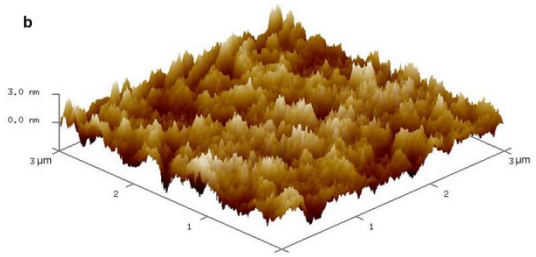

View Article Online
DOI: 10.1039/C5TA03971A

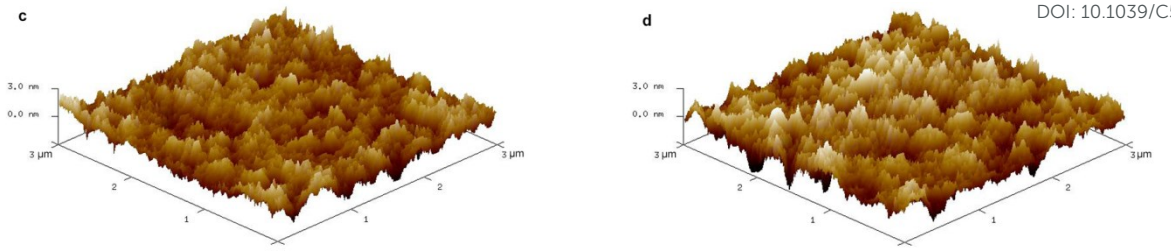

Fig. 6 AFM 3D graph of ASQ-5/$PC_{71}BM$ blend films (a, RMS=0.70 nm) and with thermal annealing (b, RMS= 0.74 nm); ASQ-5-CN/$PC_{71}BM$ blend films (c, RMS=0.71 nm) and with thermal annealing (d, RMS= 0.79 nm).

3.6 Organic solar cells

To evaluate the photovoltaic performance of ASQ-5-CN, devices with structure of ITO/MoO_3 (8 nm)/ASQ: $PC_{71}BM$ (60 nm)/BCP (6 nm)/Al (100 nm) have been fabricated. For comparison, reference devices with ASQ-5 as electron donor materials have also been fabricated under very similar conditions. The representative data of these devices were summarized in Table 4, the current density-voltage (*J-V*) curves as well as the external quantum efficiency (EQE) spectra were shown in Fig. 7. Firstly, the effect of different blend ratios of ASQ-5-CN/$PC_{71}BM$ on the photovoltaic properties of the devices were investigated. When the composition of $PC_{71}BM$ increased from 1:2 to 1:3, the J_{sc} of the device increased slightly from 10.49 to 10.77 mA cm^{-2}, but no distinct changes on both V_{oc} and FF could be observed, and the PCE of the devices was improved from 4.78% to 5.00%. With further increased blending ratio of $PC_{71}BM$ from 1:3 to 1:6, both the J_{sc} and FF of the corresponding device decreased gradually from 10.77 to 10.03 mA cm^{-2} and from 0.50 to 0.43, respectively, hence the PCE dropped to 4.05%. Therefore, the highest PCE value was obtained when ASQ-5-CN/$PC_{71}BM$ blend ratio is 1:3. It should be mentioned that when the D/A blend ratios decreased from 1:2 to 1:6, the PCE of these devices all show 4~5%, thus the photovoltaic performance of the OSC was not very sensitive to the D/A blend ratios.

Consequently, a reference ASQ-5-device with similar D/A blend ratio of 1:3 was fabricated, and the PCE, V_{oc}, J_{sc}, and FF of this device was 3.95%, 0.83 V, 10.35 mA cm^{-2}, and 0.46 in sequence, each was inferior to that of the ASQ-5-CN-device (5.00%, 0.93 V, 10.77 mA cm^{-2}, and 0.50, respectively). The 0.10 V higher V_{oc} of the ASQ-5-CN-device relative to the

reference device was consistent with the 0.11 eV decreased HOMO energy level of ASQ-5-CN than that of ASQ-5. Moreover, the ASQ-5-CN-based device also displayed a higher J_{sc} than that of the reference device. As J_{sc} should correlate highly with the light-harvesting capability, carrier mobility, and morphology of the active layer.[44-46] To elucidate the origin of the enhanced J_{sc} in ASQ-5-CN-device, the EQE curves of the two devices were recorded. As shown in Fig. 7d, in comparison with the reference device, the ASQ-5-CN-device shown narrower spectral response; but its EQE values in 300~700 nm were much higher. And the EQE data were in line with the absorption of the corresponding active layer (shown in Fig. S2, ESI). Additionally, AFM characterization results revealed that both the two blend films shown similar morphologies and smooth surfaces (Fig. 6). Thus, the increased J_{sc} of ASQ-5-CN-device should chiefly originate from the higher hole mobility of its active layer. Additionally, the FF of ASQ-5-CN-based device was also higher than that of ASQ-5 (0.50 *vs.* 0.46), which is attributed to its higher hole mobility and better balanced hole and electron mobilities.[20] It should be pointed out that the high FF of 0.50 is, to the best of our knowledge, one of the highest FF of solution-processed BHJ-OSC with squaraine derivatives as electron donor materials.

Upon thermal annealing, the performance of both the two devices was enhanced, with the best PCE of 4.22% for the reference device, and 5.24% for the ASQ-5-CN-device. The enhanced PCE should be mainly attributed to the improved J_{sc} upon thermal annealing. Because the outdoor working temperature of solar cells is generally higher than the ambient conditions, these devices were also measured at 80 °C.[47] Excitingly, for the ASQ-5-CN-device, although its V_{oc} (0.92 *vs.* 0.85 V) was found to drop slightly, both its J_{sc} (12.40 *vs.* 11.38 mA cm^{-2}) and FF (0.58 *vs.* 0.50) were observed to be significantly enhanced (Table 4), hence the PCE is as high as 6.11%, about 17% enhanced than that of the as-prepared device (5.24%), which should be attributed to the significantly enhanced hole mobility and decreased μ_e/μ_h ratio.[48] After being recooled down to room temperature, the device shown similar performance (PCE: 5.23% *vs.* 5.24%) with that of the annealed one (Table 4), which isquite promising candidates for practical applications.

View Article Online
DOI: 10.1039/C5TA03971A

Table 4 Photovoltaic performances of organic solar cells based on ASQ: $PC_{71}BM$.

Donor	Ratio (D : A)	V_{oc} [d] (V)	J_{sc} [d] (mA cm^{-2})	FF [d]	PCE [d] (%)
ASQ-5-CN	1 : 2	0.93 (0.93)	10.49 (10.53)	0.49 (0.48)	4.78 (4.70)
	1 : 3	0.93 (0.93)	10.77 (10.62)	0.50 (0.50)	5.00 (4.94)
	1 : 4	0.93 (0.93)	10.38 (10.25)	0.47 (0.47)	4.54 (4.48)
	1 : 5	0.93 (0.93)	10.14 (10.05)	0.46 (0.46)	4.34 (4.30)
	1 : 6	0.94 (0.94)	10.03 (9.90)	0.43 (0.43)	4.05 (4.00)
	1 : 3 [a]	0.92 (0.92)	11.38 (11.20)	0.50 (0.50)	5.24 (5.15)
	1 : 3 [b]	0.85 (0.85)	12.40 (12.38)	0.58 (0.57)	6.11 (6.00)
	1 : 3 [c]	0.92 (0.92)	11.37 (11.13)	0.50 (0.50)	5.23 (5.12)
ASQ-5	1 : 3	0.83 (0.83)	10.35 (10.16)	0.46 (0.46)	3.95 (3.88)
	1 : 3 [a]	0.82 (0.82)	10.94 (10.79)	0.47 (0.47)	4.22 (4.16)

[a] Tested at room temperature after having been thermally annealed at 80 °C for 10 min; [b] tested at 80 °C; [c] tested after being recooled down to room temperature; [d] the first values are the best data obtained; the values in parentheses are average values from 8 devices.

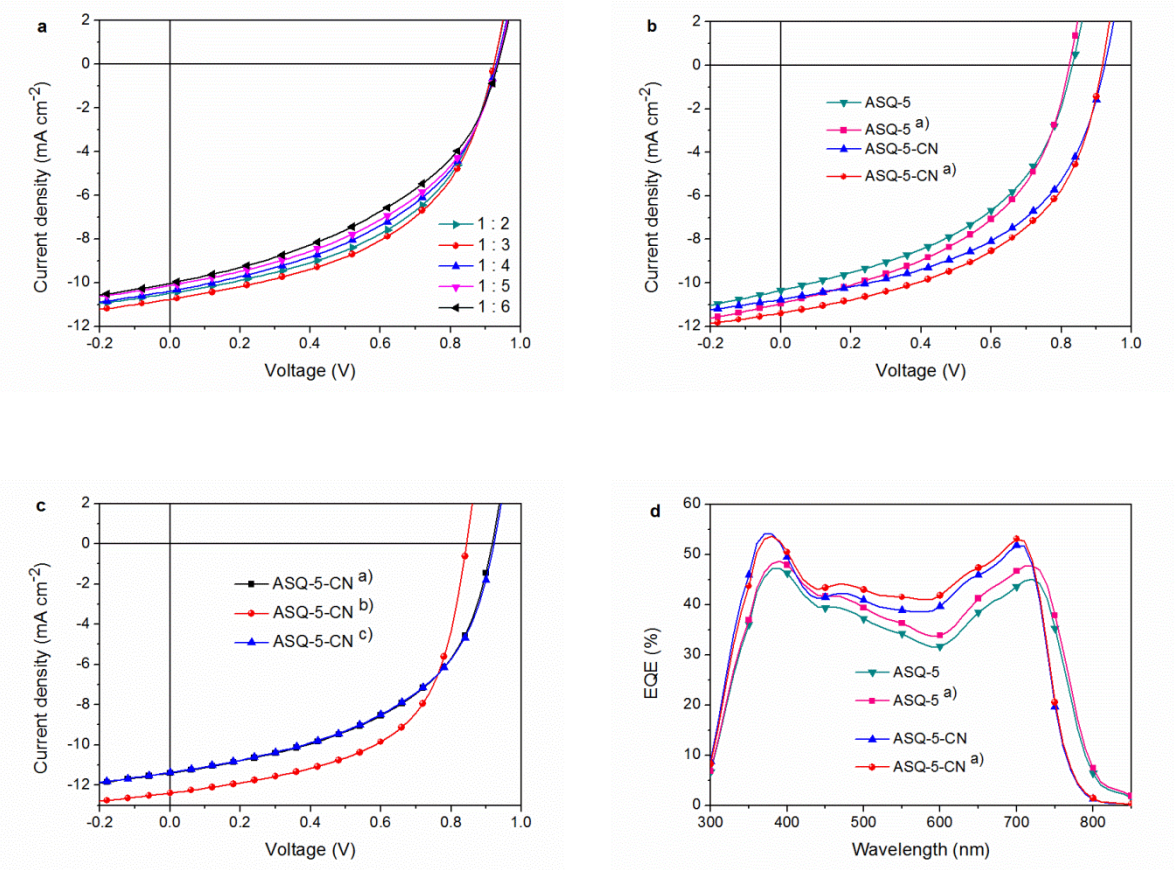

Fig. 7 a) *J-V* curve characteristics of ASQ-5-CN-based devices with different ASQ-5-CN /$PC_{71}BM$ blend ratios; b) *J-V* curve characteristics of ASQ-5-CN and ASQ-5 devices (D/A =

1/3); c) *J-V* curve characteristics of ASQ-5-CN devices (D/A = 1/3) under different measure conditions; and d) EQE curves of the ASQ-5-CN and ASQ-5 devices with D/A ratio of 1:3. [a)] Devices tested at room temperature after having been thermally annealed at 80 °C for 10 min; [b)] device tested at 80 °C; [c)] devices tested after being recooled down to room temperature.

4. Conclusion

In conclusion, cyano-substitution on the electron-donating indoline end-capper of ASQ-5, the resulted asymmetrical squaraine ASQ-5-CN could possessed comparable absorption characteristic with ASQ-5 in thin film states, but lower HOMO energy level relative to ASQ-5. In addition to its 0.11 V lowered HOMO energy level, ASQ-5-CN could show much enhanced dipole-dipole interaction than that of ASQ-5, hence higher hole mobility could be acquired in ASQ-5-CN. Consequently, in comparison with that of ASQ-5-based reference device, solution-processed ASQ-5-CN-based BHJ-OSC shown simultaneously enhanced V_{oc}, J_{sc} and FF, and a high PCE of 6.11% could be achieved, which is the best PCE of solution-processed BHJ-OSC based on squaraine materials reported so far. Our results show the importance of molecular tailoring for achieving high performance photovoltaic materials, and the cyano-substitution on the end-capper of conjugated small molecules may be an important strategy for achieving high performance photovoltaic devices with greatly improved V_{oc}, J_{sc} and FF.

Acknowledgements

We acknowledge the financial support for this work by the National Natural Science Foundation of China (project No. 21190031, 21372168 and 21432005) and China Scholarship Council. We are grateful to the Comprehensive Training Platform of Specialized Laboratory, College of Chemistry, Sichuan University for providing NMR and HR-MS data for the intermediates and objective compounds.

View Article Online
DOI: 10.1039/C5TA03971A

References

[1] B. Kan, Q. Zhang, M. Li, X. Wan, W. Ni, G. Long, Y. Wang, X. Yang, H. Feng and Y. Chen, *J. Am. Chem. Soc.*, 2014, **136**, 15529-15532.

[2] Q. Zhang, B. Kan, F. Liu, G. Long, X. Wan, X. Chen, Y. Zuo, W. Ni, H. Zhang, M. Li, Z. Hu, F. Huang, Y. Cao, Z. Liang, M. Zhang, T. P. Russell and Y. Chen, *Nat. Photon.*, 2015, **9**, 35-41.

[3] Z. He, B. Xiao, F. Liu, H. Wu, Y. Yang, S. Xiao, C. Wang, T. P. Russell and Y. Cao, *Nat. Photon.*, 2015, **9**, 174-179.

[4] K. A. Mazzio and C. K. Luscombe, *Chem. Soc. Rev.*, 2015, **44**, 78-90.

[5] J. Roncali, P. Leriche and P. Blanchard, *Adv. Mater.*, 2014, **26**, 3821-3838.

[6] J.-L. Wang, Q.-R. Yin, J.-S. Miao, Z. Wu, Z.-F. Chang, Y. Cao, R.-B. Zhang, J.-Y. Wang, H.-B. Wu and Y. Cao, *Adv. Funct. Mater.*, 2015, **25**, 3514-3523.

[7] J.-L. Wang, Z. Wu, J.-S. Miao, K.-K. Liu, Z.-F. Chang, R.-B. Zhang, H.-B. Wu and Y. Cao, *Chem. Mater.*, 2015, **27**, 4338-4348.

[8] U. Mayerhöffer, K. Deing, K. Gruβ, H. Braunschweig, K. Meerholz and F. Würthner, *Angew. Chem. Int. Ed.*, 2009, **48**, 8776-8779.

[9] D. Bagnis, L. Beverina, H. Huang, F. Silvestri, Y. Yao, H. Yan, G. A. Pagani, T. J. Marks and A. Facchetti, *J. Am. Chem. Soc.*, 2010, **132**, 4074-4075.

[10] S. Wang, L. Hall, V. V. Diev, R. Haiges, G. Wei, X. Xiao, P. I. Djurovich, S. R. Forrest and M. E. Thompson, *Chem. Mater.*, 2011, **23**, 4789-4798.

[11] G. Wei, X. Xiao, S. Wang, K. Sun, K. J. Bergemann, M. E. Thompson and S. R. Forrest, *ACS Nano*, 2012, **6**, 972-978.

[12] J.-S. Huang, T. Goh, X. Li, M. Y. Sfeir, E. A. Bielinski, S. Tomasulo, M. L. Lee, N. Hazari and A. D. Taylor, *Nat. Photon.*, 2013, **7**, 479-485.

[13] G. Chen, H. Sasabe, Y. Sasaki, H. Katagiri, X.-F. Wang, T. Sano, Z. Hong, Y. Yang and J. Kido, *Chem. Mater.*, 2014, **26**, 1356-1364.

[14] A.Viterisi, N. F. Montcada, C. V. Kumar, F. Gispert-Guirado, E. Martin, E. Escudero and E. Palomares, *J. Mater. Chem. A*, 2014, **2**, 3536-3542.

[15] H. Sasabe, T. Igrashi, Y. Sasaki, G. Chen, Z. Hong and J. Kido, *RSC Adv.*, 2014, **4**, 42804-42807.

[16] T. Goh, J.-S. Huang, E. A. Bielinski, B. A. Thompson, S. Tomasulo, M. L. Lee, M. Y. Sfeir, N. Hazari and A. D. Taylor, *ACS Photon.*, 2015, **2**, 86-95.

[17] L. Beverina and P. Salice, *Eur. J. Org. Chem.*, 2010, **2010**, 1207-1225.

[18] Y. Chen, Y. Zhu, D. Yang, Q. Luo, L. Yang, Y. Huang, S. Zhao and Z. Lu, *Chem. Commun.*, 2015, **51**, 6133-6136.

[19] S. Paek, H. Choi, H. Jo, K. Lee, K. Song, S. A. Siddiqui, G. D. Sharma and J. Ko, *J. Mater. Chem. C*, 2015, **3**, 7029-7037.

[20] D. Yang, L. Yang, Y. Huang, Y. Jiao, T. Igarashi, Y. Chen, Z. Lu, X. Pu, H. Sasabe and J. Kido, *ACS Appl. Mater. Interfaces*, 2015, **7**, 13675-13684.

[21] G. Wei, S. Wang, K. Sun, M. E. Thompson and S. R. Forrest, *Adv. Energy Mater.*, 2011, **1**, 184-187.

[22] J. Fabian, H. Nakazumi and M. Matsuoka, *Chem. Rev.*, 1992, **92**, 1197-1226.

[23] S. S. Pandey, R. Watanabe, N. Fujikawa, Y. Ogomi, Y. Yamaguchi and S. Hayase, *Proc. SPIE* 2011, **8111**, 811116.

[24] D. Yang, Q. Yang, L. Yang, Q. Luo, Y. Huang, Z. Lu and S. Zhao, *Chem. Commun.*, 2013, **49**, 10465-10467.

[25] D. Yang, Q. Yang, L. Yang, Q. Luo, Y. Chen, Y. Zhu, Y. Huang, Z. Lu and S. Zhao, *Chem. Commun.*, 2014, **50**, 9346-9348.

[26] L. Yang, Q. Yang, D. Yang, Q. Luo, Y. Zhu, Y. Huang, S. Zhao and Z. Lu, *J. Mater. Chem. A*, 2014, **2**, 18313-18321.

[27] D. Yang, Y. Zhu, Y. Jiao, Q. Yang, L. Yang, Q. Luo, X. Pu, Y. Huang, S. Zhao and Z. Lu, *RSC Adv.*, 2015, **5**, 20724-20733.

[28] X. Liu, M. Li, R. He and W. Shen, *Phys. Chem. Chem. Phys.*, 2014, **16**, 311-323.

[29] S. Zeng, L. Yin, C. Ji, X. Jiang, K. Li, Y. Li and Y. Wang, *Chem. Commun.*, 2012, **48**, 10627-10629.

[30] H. Cha, H. N. Kim, T. K. An, M. S. Kang, S.-K. Kwon, Y.-H. Kim and C. E. Park, *ACS Appl. Mater. Interfaces*, 2014, **6**, 15774-15782.

[31] B. C. Thompson, Y.-G. Kim and J. R. Reynolds, *Macromolecules*, 2005, **38**, 5359-5362.

[32] J. A. Mikroyannidis, M. M. Stylianakis, P. Suresh, P. Balraju and G. D. Sharma, *Org. Electron.*, 2009, **10**, 1320-1333.

[33] G. D. Sharma, J. A. Mikroyannidis, R. Kurchania and K. R. J. Thomas, *J. Mater. Chem.* 2012, **22**, 13986-13995.

[34] M. Singh, R. Kurchania, J. A. Mikroyannidis, S. S. Sharma and G. D. Sharma, *J. Mater. Chem. A*, 2013, **1**, 2297-2306.

[35] G. L. Schulz, M. Löbert, I. Ata, M. Urdanpilleta, M. Lindén, A. Mishra and P. Bäuerle, *J. Mater. Chem. A*, 2015, **3**, 13738-13748.

[36] Y. Liu, J. Zhou, X. Wan and Y. Chen, *Tetrahedron*, 2009, **65**, 5209-5215.

[37] A. Srikrishna, T. J. Reddy and R. Viswajanani, *Tetrahedron*, 1996, **52**, 1631-1636.

[38] Y. Li, *Acc. Chem. Res.*, 2011, **45**, 723-733.

[39] M. C. Scharber, D. Muhlbacher, M. Koppe, P. Denk, C. Waldauf, A. J. Heeger and C. J. Brabec, *Adv. Mater.*, 2006, **18**, 789-794.

[40] H. Bürckstümmer, E. V. Tulyakova, M. Deppisch, M. R. Lenze, N. M. Kronenberg, M. Gsänger, M. Stolte, K. Meerholz and F. Würthner, *Angew. Chem. Int. Ed.*, 2011, **50**, 11628-11632.

[41] C. J. Takacs, Y. Sun, G. C. Welch, L. A. Perez, X. Liu, W. Wen, G. C. Bazan and A. J. Heeger, *J. Am. Chem. Soc.*, 2012, **134**, 16597-16606.

[42] A. Liess, L. Huang, A. Arjona-Esteban, A. Lv, M. Gsänger, V. Stepanenko, M. Stolte and F. Würthner, *Adv. Funct. Mater.*, 2015, **25**, 44-57.

[43] Z. He, C. Zhong, X. Huang, W. Y. Wong, H. Wu, L. Chen, S. Su and Y. Cao, *Adv. Mater.*, 2011, **23**, 4636-4643.

[44] H. Hoppe, M. Niggemann, C. Winder, J. Kraut, R. Hiesgen, A. Hinsch, D. Meissner and N. S. Sariciftci, *Adv. Funct. Mater.*, 2004, **14**, 1005-1011.

[45] V. D. Mihailetchi, H. X. Xie, B. de Boer, L. J. A. Koster and P. W. M. Blom, *Adv. Funct. Mater.*, 2006, **16**, 699-708.

[45] A. J. Heeger, *Adv. Mater.*, 2014, **26**, 10-28.

[47] G. Chen, H. Sasabe, Z. Wang, X. F. Wang, Z. Hong, Y. Yang and J. Kido, *Phys. Chem. Chem. Phys.*, 2012, **14**, 14661-14666.

[48] B. Yang, J. Cox, Y. Yuan, F. Guo and J. Huang, *Appl. Phys. Lett.*, 2011, **99**, 133302.

View Article Online
DOI: 10.1039/C5TA03971A

Abstract Graph

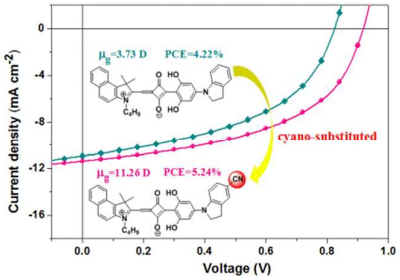

Textual Abstract

Novel asymmetrical squaraine bearing cyano-substituted indoline end-capping group for solution-processed organic solar cells with high V_{oc} and PCE was synthesized.